Turbulence modelling for flows with strong variations in thermo-physical properties

Otero Rodriguez, Gustavo; Patel, Ashish; Diez Sanhueza, Rafael; Pecnik, Rene

DOI
10.1016/j.ijheatfluidflow.2018.07.005

Publication date
2018

Document Version
Accepted author manuscript

Published in
International Journal of Heat and Fluid Flow

Turbulence modelling for flows with strong variations in thermo-physical properties

Gustavo J. Otero R., Ashish Patel, Rafael Diez S., Rene Pecnik*

Process and Energy Department, Delft University of Technology, Leeghwaterstraat 39, 2628 CB Delft, the Netherlands

Abstract

This paper presents a novel methodology for improving eddy viscosity models in predicting wall-bounded turbulent flows with strong gradients in the thermo-physical properties. Common turbulence models for solving the Reynolds-averaged Navier-Stokes equations do not correctly account for variations in transport properties, such as density and viscosity, which can cause substantial inaccuracies in predicting important quantities of interest, for example, heat transfer and drag. Based on the semi-locally scaled turbulent kinetic energy equation, introduced in [Pecnik and Patel, J. Fluid Mech. (2017), vol. 823, R1], we analytically derive a modification of the diffusion term of turbulent scalar equations. The modification has been applied to five common eddy viscosity turbulence models and tested for fully developed turbulent channels with isothermal walls that are volumetrically heated, either by a uniform heat source or viscous heating in supersonic flow conditions. The agreement with results obtained by direct numerical simulation shows that the modification significantly improves results of eddy viscosity models for fluids with variable transport properties.

Keywords: RANS turbulence modelling, compressible flow, varying properties, semi-local scaling

1. Introduction

Turbulence plays a vital role in heat transfer and skin friction across the boundary layer in wall bounded flows. For engineers, it is therefore of paramount importance to accurately model turbulence during the design process of any flow guiding devices, such as heat exchangers with strongly cooled or heated flows, rocket propulsion systems, combustion chambers with chemically reacting flows, or turbomachinery flows with unconventional working fluids. In all these applications, strong heat transfer causes large temperature gradients and consequently large variations in density, viscosity, thermal conductivity, heat capacity, etc., which alter the conventional behavior of turbulence. Despite decades of research, turbulent flows with variable thermophysical properties are still far from being understood. Accordingly, turbulence models for engineering applications with large heat transfer rates are not able to provide accurate results for Nusselt numbers, pressure losses, or any other quantities of interest.

In the past, experiments and direct numerical simulations (DNS) have been performed to study turbulent flows over a wide range of Reynolds numbers for boundary layers, channel, pipes, among others [1, 2, 3, 4]. However, these detailed measurements and simulations are limited to simple geometries, and as the Reynolds number increases, DNS become computationally more expensive. Because of this fact, turbulence models for simulations of the Reynolds-averaged Navier-Stokes (RANS) equations rely on a limited number of accurate data, and their development is additionally hampered by the lack of knowledge on how turbulence is affected by strong variations of thermophysical properties. Since almost all turbulence models have been developed for incompressible flows, several extensions to include compressible effects have been proposed in the past by [5, 6, 7]. For example, if the turbulent kinetic energy (TKE) equation is derived on the basis of the compressible Navier-Stokes equations, additional terms appear, i.e. pressure -work and -dilatation, dilatational dissipation, and additional terms related to fluctuations of density, velocity, pressure, etc. The modification of the TKE in flows with strong heat transfer has been attributed to these terms and according models have been proposed in the past [6, 7, 8]. Huang, Bradshaw, and Coakley [5], analyzed the log-layer behaviour of a compressible boundary layer using turbulence models and claimed that the model closure coefficients must be a function of mean density gradients to satisfy the law-of-the-wall obtained with the van Driest velocity transformation [9].

A different approach to sensitize turbulence models for compressible flows with large density variations, was proposed by Catris and Aupoix [10]. They used the formulation developed by Huang *et al.* [5] for the closure coefficients, to modify the diffusion term of the turbulent dissipation transport equation. Additionally, they argued that the diffusion of TKE acts upon the energy per unit volume $[(kg\ m^2/s^2)/m^3]$ of turbulent fluctuations, which

*Corresponding author
Email address: `r.pecnik@tudelft.nl` (Rene Pecnik)
URL: `http://dutw1479.wbmt.tudelft.nl/~renep/` (Rene Pecnik)

Nomenclature

$\check{\nu}$	Spalart-Allmaras eddy viscosity
δ_v	Viscous length scale
δ_{ij}	Kronecker delta
γ	Heat capacity ratio
κ	Von Karman constant (= 0.41)
λ	Thermal conductivity
μ	Dynamic viscosity
μ_t	Eddy viscosity
ω	Specific turbulent dissipation
Φ	Volumetric source term
ρ	Density
σ	Model constant
τ	Shear stress
ε	Turbulent dissipation
c_p	Isobaric heat capacity
Ec_τ	Friction based Eckert number ($= u_\tau^2/(\tilde{T}_w \tilde{c}_{p,w})$)
f_x	External body force
H	Enthalpy
h	Characteristic length, half channel height
k	Turbulent kinetic energy ($= u_i''u_i''/2$)
M_τ	Friction based Mach number
p	Pressure
P_k	Production of turbulent kinetic energy
Pr	Prandlt number ($= c_p\mu/\lambda$)
Pr_t	Turbulent Prandlt number
R	Specific gas constant
Re_τ	Friction Reynolds number ($= u_\tau \rho_w h/\mu_w$)
$Re_\tau^\star$	Semi-local Reynolds number
Re_b	Bulk Reynolds number ($= u_b h \rho_b/\mu_w$)
T	Temperature
t	Time
u	Velocity
$u^\star$	Universal velocity transformation ($= \int_0^{u^{vD}} \left[1 + (y/Re_\tau^\star)\, \partial Re_\tau^\star/\partial y\right] \partial u^{vD}$)
u^{vD}	Van Driest velocity transformation ($= \int_0^{(u/u_\tau)} \sqrt{\rho/\rho_w}\, \partial\left(u/u_\tau\right)$)
u_τ	Friction velocity ($= \sqrt{\tau_w/\rho_w}$)
$u_\tau^\star$	Semi-local friction velocity ($= \sqrt{\tau_w/\langle\rho\rangle}$)
x	Length
y^+	Locally scaled wall distance ($= y\ Re_\tau/h$)
$y^\star$	Semi-locally scaled wall distance ($= y\ Re_\tau^\star/h$)

Accents and subscripts

$\tilde{\phi}$	Dimensional quantity
ϕ	Locally scaled quantity
$\hat{\phi}$	Semi-locally scaled quantity
ϕ_b	Bulk quantity
ϕ_c	Quantity at the channel center
ϕ_w	Quantity at the wall

Averaging operators

$\langle\cdot\rangle$	Reynolds averaged $\phi = \langle\phi\rangle + \phi'$ with $\langle\phi'\rangle = 0$
$\{\cdot\}$	Favre averaged $\phi = \{\phi\} + \phi''$ with $\langle\rho\rangle\{\phi\} = \langle\rho\phi\rangle$, $\{\phi''\} = 0$ and $\langle\phi''\rangle \neq 0$

can be expressed as ρk. The diffusion of TKE is therefore based on ρk, while the diffusion coefficient is divided by the density on the basis of dimensional consistency. Their approach improved eddy viscosity models for supersonic adiabatic boundary layer flows, without including the additional compressibility terms. However, these ad-hoc corrections to the TKE equations need to be assessed for a wide range of flows, including standard low-speed flows [11] and free shear flows [12].

In this study, we analytically derive modifications of eddy viscosity models for flows with strong property variations, which are based on the fact that the "leading-order effect" of variable properties on wall bounded turbulence can be characterized by the semi-local Reynolds number only [13, 14]. The developed methodology is generic and applicable to a wide range of eddy viscosity models. To demonstrate the improvement, we have applied the modifications to five different EVM from literature [15, 16, 17, 18, 19] and compared the results to direct numerical simulations of heated fully developed turbulent channel flows with varying thermo-physical properties [14, 20]. Furthermore, the density corrections proposed by Catris and Aupoix [10] has been considered as well. The matlab source code used in this paper and the DNS data from [14] are available on GitHub [21].

2. SLS turbulence modelling

The semi-local scaling (SLS) as proposed by Huang *et al.* in 1995 [8], is based on the wall shear stress $\tilde{\tau}_w$ and on local mean (instead of wall) quantities of den-

Table 1: Comparison of local, ϕ, and semi-local, $\hat{\phi}$, scaling for the most relevant quantities. The dimensional quantities are expressed as $\tilde{\phi}$. The subscript w indicates the averaged wall value, which is used in the present study as the reference condition for the local scaling. The friction velocity is used for scaling the velocity. The characteristic length, $\tilde{h}$, is the half channel height in our study.

Quantity			Local scaling		Semi-local sc.
Length	$\tilde{x}_i$	=	$x_i \tilde{h}$	=	$\hat{x}_i \tilde{h}$
Velocity	$\tilde{u}$	=	$u u_\tau$	=	$\hat{u} u_\tau^\star$
Pressure	$\tilde{p}$	=	$p \tilde{\rho}_w u_\tau^2$	=	$\hat{p} \langle \tilde{\rho} \rangle {u_\tau^\star}^2$
Density	$\tilde{\rho}$	=	$\rho \tilde{\rho}_w$	=	$\hat{\rho} \langle \tilde{\rho} \rangle$
Dyn. viscosity	$\tilde{\mu}$	=	$\mu \tilde{\mu}_w$	=	$\hat{\mu} \langle \tilde{\mu} \rangle$
Eddy viscosity	$\tilde{\mu}_t$	=	$\mu_t \tilde{\rho}_w \tilde{h} u_\tau$	=	$\hat{\mu}_t \langle \tilde{\rho} \rangle \tilde{h} u_\tau^\star$
TKE	$\tilde{k}$	=	$k u_\tau^2$	=	$\hat{k} {u_\tau^\star}^2$
Turb. diss.	$\tilde{\varepsilon}$	=	$\varepsilon u_\tau^3 / \tilde{h}$	=	$\hat{\varepsilon} {u_\tau^\star}^3 / \tilde{h}$
Spec. turb. diss.	$\tilde{\omega}$	=	$\omega u_\tau / \tilde{h}$	=	$\hat{\omega} u_\tau^\star / \tilde{h}$
Wall distance	$\tilde{y}$	=	$y^+ \tilde{h} / Re_\tau$	=	$y^\star \tilde{h} / Re_\tau^\star$

sity and viscosity to account for changes in viscous scales due to mean variations in the thermo-physical properties. The aim of the SLS was to collapse turbulence statistics for compressible flows at high Mach numbers with those of incompressible flows. In the SLS framework, the friction velocity and viscous length scale are defined as $u_\tau^\star = \sqrt{\tilde{\tau}_w / \langle \tilde{\rho} \rangle}$ and $\delta_v^\star = \langle \tilde{\mu} \rangle / \langle \tilde{\rho} \rangle u_\tau^\star$, respectively, where $\langle \cdot \rangle$ indicates Reynolds averaging. Accordingly, the semi-local wall distance can be defined as $y^* = \tilde{y}/\delta_v^\star$ and the semi-local Reynolds number as,

$$Re_\tau^\star = \frac{u_\tau^\star \langle \tilde{\rho} \rangle \tilde{h}}{\langle \tilde{\mu} \rangle} = \sqrt{\frac{\langle \tilde{\rho} \rangle}{\tilde{\rho}_w}} \frac{\tilde{\mu}_w}{\langle \tilde{\mu} \rangle} Re_\tau, \tag{1}$$

where $Re_\tau = u_\tau \tilde{\rho}_w \tilde{h} / \tilde{\mu}_w$ and $u_\tau = \sqrt{\tilde{\tau}_w / \tilde{\rho}_w}$, are the conventional friction Reynolds number and friction velocity based on viscous wall units. In general, any flow variable can be non-dimensionalized using wall based units and semi-local units. This is outlined in more detail in table 1. It is important to note, that the friction velocities of both scaling are related through the wall shear stress by $\tilde{\tau}_w = \tilde{\rho}_w u_\tau^2 = \langle \tilde{\rho} \rangle u_\tau^{\star 2}$. This relation will be used frequently throughout the paper.

Instead of exclusively using the semi-local scaling to collapse turbulence statistics for compressible flows with different Mach numbers, Pecnik and Patel [13] extended the use of the scaling to derive an alternative form of the TKE equation for wall-bounded flows with a strong wall-normal variations of density and viscosity. Starting from the semi-locally scaled non-conservative form of the momentum equations, and with the assumption that the wall shear stress $\tilde{\tau}_w$ changes slowly in the streamwise direction, the SLS TKE equation reads,

$$t_\tau^\star \frac{\partial \{\hat{k}\}}{\partial \tilde{t}} + \frac{\partial \{\hat{k}\}\{\hat{u}_j\}}{\partial \hat{x}_j} = \hat{P}_k - \hat{\varepsilon}_k + \hat{T}_k + \hat{C}_k + \hat{\mathcal{D}}_k, \tag{2}$$

with production $\hat{P}_k = -\{\hat{u}_i'' \hat{u}_j''\} \partial \{u_i^{vD}\} / \partial \hat{x}_j$, dissipation per unit volume $\hat{\varepsilon}_k = \langle \hat{\tau}_{ij}' \partial \hat{u}_i' / \partial \hat{x}_j \rangle$, diffusion (containing viscous diffusion, turbulent transport, and pressure diffusion) $\hat{T}_k = \partial (\langle \hat{u}_i' \hat{\tau}_{ij}' \rangle - \{\hat{u}_j'' \hat{k}\} - \langle \hat{p}' \hat{u}_j' \rangle) / \partial \hat{x}_j$, and compressibility $\hat{C}_k = \langle \hat{p}' \partial \hat{u}_j' / \partial \hat{x}_j \rangle - \langle \hat{u}_j'' \rangle \partial \langle \hat{p} \rangle / \partial \hat{x}_j + \langle \hat{u}_i'' \rangle \partial \langle \hat{\tau}_{ij} \rangle / \partial \hat{x}_j$. $\hat{\tau}_{ij} = \hat{\mu} / Re_\tau^\star [(\partial \hat{u}_i / \partial \hat{x}_j + \partial \hat{u}_j / \partial \hat{x}_i) - 2/3 (\partial \hat{u}_k / \partial \hat{x}_k) \delta_{ij}]$ is the shear stress tensor.

Due to the semi-local scaling, additional terms appear in equation (2), which are lumped in $\hat{\mathcal{D}}_k = (\{\hat{u}_j\}\{\hat{k}\} + \{\hat{u}_j'' \hat{k}\}) d_j - \langle \hat{u}_i'' \, \partial \hat{D}_{ij} / \partial \hat{x}_j \rangle$, with

$$\hat{D}_{ij} = \frac{\hat{\mu}}{Re_\tau^\star} \left[(\hat{u}_i d_j + \hat{u}_j d_i) - \frac{2}{3} \hat{u}_k d_k \delta_{ij} \right],$$

$d_i = 1/2 \langle \rho \rangle^{-1} \partial \langle \rho \rangle / \partial \hat{x}_i$ and δ_{ij} the Kronecker delta. The mean density gradient appears since the turbulent kinetic energy (and/or the velocity) within the derivatives is scaled by the semi-local friction velocity $u_\tau^\star$. For example, taking the derivative of $u_\tau^\star$, one can write (assuming that the averaged wall shear stress is constant),

$$\frac{\partial u_\tau^\star}{\partial \hat{x}_i} = \sqrt{\tau_w} \frac{\partial \sqrt{1/\langle \rho \rangle}}{\partial \hat{x}_i} = \sqrt{\tau_w} \frac{\partial \sqrt{1/\langle \rho \rangle}}{\partial \langle \rho \rangle} \frac{\partial \langle \rho \rangle}{\partial \hat{x}_i}$$
$$= -\frac{1}{2} \frac{u_\tau^\star}{\langle \rho \rangle} \frac{\partial \langle \rho \rangle}{\partial \hat{x}_i} = -u_\tau^\star d_i.$$

The curly brackets $\{\cdot\}$ indicate Favre averaging and $t_\tau^\star = \tilde{h}/u_\tau^\star$. It is important to mention that the Favre averaged TKE is defined as $\{\hat{k}\} = \langle \hat{\rho} \hat{k} \rangle / \langle \hat{\rho} \rangle$, which, with the Reynolds decomposition of the locally scaled density as $\langle \hat{\rho} \rangle = \langle \tilde{\rho} \rangle / \langle \tilde{\rho} \rangle + \langle \tilde{\rho}' \rangle / \langle \tilde{\rho} \rangle = 1$, can also be expressed as $\{\hat{k}\} = \langle \hat{\rho} \hat{k} \rangle = \langle \hat{\rho} \hat{u}_i'' \hat{u}_i'' \rangle / 2$. This relation $\{\phi\} = \langle \hat{\rho} \phi \rangle$ will be used frequently in this paper as well. The reader is referred to Pecnik and Patel [13] for more details on eq. (2) and its derivation.

The most important findings in Pecnik and Patel [13] are that effects of property variations on turbulence can be characterized by gradients of the semi-local Reynolds number $Re_\tau^\star$, and that the turbulent production is governed by the gradient of the van Driest velocity increment, defined as $\partial \{u^{vD}\} = \sqrt{\langle \tilde{\rho} \rangle / \tilde{\rho}_w} \partial (\{\tilde{u}\}/u_\tau)$. Moreover, for the cases investigated in [13], it appears that the terms related to compressible effects and mean density gradients, $\hat{C}_k$ and $\hat{\mathcal{D}}_k$, respectively, have a minor effect on the evolution of the SLS TKE.

In the present study, we intend to leverage the knowledge gained from the SLS TKE equation to improve turbulence models predictions of wall-bounded turbulent flows with strong gradients in the thermo-physical properties. As such, we first obtain a closed form of the exact SLS TKE equation, eq. (2), which is then scaled back to conventional (wall based) scales.

For the purpose of obtaining a closed form of the SLS TKE equation, the following assumptions are applied. The production of TKE is estimated using the Boussinesq approximation by modelling the turbulent shear stress. Additionally, it is assumed that the total diffusion $\hat{T}_k$ can be modelled using the gradient diffusion hypothesis [22], and that the dynamic viscosity fluctuations are negligible compared to its averaged counterpart ($\tilde{\mu}' \ll \langle\tilde{\mu}\rangle$). As such, the semi-locally scaled dynamic viscosity is equal to $\langle\hat{\mu}\rangle = \langle\tilde{\mu}/\langle\tilde{\mu}\rangle\rangle = 1$. Finally, neglecting $\hat{C}_k$ and $\hat{\mathcal{D}}_k$, as they have a minor effect, the SLS TKE equation can then be written as

$$t_\tau^\star \frac{\partial\{\hat{k}\}}{\partial \tilde{t}} + \frac{\partial\{\hat{k}\}\{\hat{u}_j\}}{\partial \hat{x}_j} = \hat{P}_k - \hat{\varepsilon} + \frac{\partial}{\partial \hat{x}_j}\left[\left(\frac{1}{Re_\tau^\star} + \frac{\hat{\mu}_t}{\sigma_k}\right)\frac{\partial\{\hat{k}\}}{\partial \hat{x}_j}\right]. \quad (3)$$

If this form of the TKE equation is used in conjunction with an eddy viscosity turbulence model, the results for turbulent flows with large thermophysical property variations significantly improve [13]. However, for general industrial applications with complex geometries, it is not feasible to solve the semi-locally scaled equations. The reason is that all turbulence variables would need to be rescaled every iteration step by quantities that depend on the wall friction at the closest wall and by local quantities of density and viscosity.

To overcome this, the focus of the derivation in this paper is to transform equation (3) back to conventional scales, in particular viscous wall units. The scaling transformations outlined in table 1 will be used for each term in (3). Starting with the turbulent kinetic energy,

$$\begin{aligned}\{\hat{k}\} &= \langle\hat{\rho}\hat{u}_i''\hat{u}_i''\rangle/2 = \left\langle \rho\frac{\tilde{\rho}_w}{\langle\tilde{\rho}\rangle}u_i''\frac{u_\tau}{u_\tau^\star}u_i''\frac{u_\tau}{u_\tau^\star}\right\rangle/2 \\ &= \left\langle \rho\frac{\tilde{\rho}_w}{\langle\tilde{\rho}\rangle}u_i''\sqrt{\frac{\langle\tilde{\rho}\rangle}{\tilde{\rho}_w}}u_i''\sqrt{\frac{\langle\tilde{\rho}\rangle}{\tilde{\rho}_w}}\right\rangle/2 = \langle\rho u_i''u_i''\rangle/2 \\ &= \langle\rho k\rangle = \langle\rho\rangle\{k\}.\end{aligned}$$

Then, we obtain for the time derivative the following:

$$t_\tau^\star\frac{\partial\{\hat{k}\}}{\partial\tilde{t}} = t_\tau^\star\frac{\partial\langle\rho\rangle\{k\}}{\partial\tilde{t}}.$$

The convective term transforms into,

$$\begin{aligned}\frac{\partial\{\hat{k}\}\{\hat{u}_j\}}{\partial\hat{x}_j} &= \frac{\tilde{h}}{\tilde{h}}\frac{\partial}{\partial x_j}\left[\langle\rho\rangle\{k\}\{u_j\}\sqrt{\frac{\langle\tilde{\rho}\rangle}{\tilde{\rho}_w}}\right] \\ &= \frac{\partial}{\partial x_j}\left[\langle\rho\rangle^{1.5}\{k\}\{u_j\}\right] = \frac{\partial\sqrt{\langle\rho\rangle}\langle\rho\rangle\{k\}\{u_j\}}{\partial x_j} \\ &= \sqrt{\langle\rho\rangle}\left(\frac{\partial\langle\rho\rangle\{k\}\{u_j\}}{\partial x_j} + \frac{\langle\rho\rangle\{k\}\{u_j\}}{2\langle\rho\rangle}\frac{\partial\langle\rho\rangle}{\partial x_j}\right).\end{aligned}$$

As it can be seen, the convection now consists of two terms. However, the second term is a mathematical artefact, which can be canceled by one of the terms in $\hat{\mathcal{D}}_k$. The production of TKE transformed back to a scaling based on wall units, results in

$$\begin{aligned}\hat{P}_k &= -\{\hat{u}_i''\hat{u}_j''\}\frac{\partial\{u^{vD}\}}{\partial\hat{x}_j} = -\langle\hat{\rho}\hat{u}_i''\hat{u}_j''\rangle\frac{\partial\{u^{vD}\}}{\partial x_j} \\ &= -\left\langle\rho\frac{\tilde{\rho}_w}{\langle\tilde{\rho}\rangle}u_i''\sqrt{\frac{\langle\tilde{\rho}\rangle}{\tilde{\rho}_w}}u_j''\sqrt{\frac{\langle\tilde{\rho}\rangle}{\tilde{\rho}_w}}\right\rangle\sqrt{\frac{\langle\tilde{\rho}\rangle}{\tilde{\rho}_w}}\frac{\partial\{u\}}{\partial x_j} \\ &= \sqrt{\langle\rho\rangle}\left(-\langle\rho u_i''u_j''\rangle\frac{\partial\{u\}}{\partial x_j}\right) = \sqrt{\langle\rho\rangle}P_k.\end{aligned} \quad (4)$$

The transformation applied for the turbulent dissipation gives,

$$\hat{\varepsilon} = \varepsilon\left(\frac{u_\tau/\tilde{h}}{u_\tau^\star/\tilde{h}}\right)^3 = \varepsilon\left(\frac{\langle\tilde{\rho}\rangle}{\tilde{\rho}_w}\right)^{1.5} = \sqrt{\langle\rho\rangle}\langle\rho\rangle\varepsilon.$$

The semi-locally scaled dynamic viscosity and eddy viscosity can also be written as,

$$\frac{1}{Re_\tau^\star} = \frac{1}{Re_\tau}\sqrt{\frac{\tilde{\rho}_w}{\langle\tilde{\rho}\rangle}}\frac{\langle\tilde{\mu}\rangle}{\tilde{\mu}_w} = \frac{1}{\sqrt{\langle\rho\rangle}}\frac{\langle\mu\rangle}{Re_\tau},$$

and,

$$\frac{\hat{\mu}_t}{\sigma_k} = \frac{\mu_t}{\sigma_k}\frac{\tilde{\rho}_w\tilde{h}u_\tau}{\langle\tilde{\rho}\rangle\tilde{h}u_\tau^\star} = \frac{\mu_t}{\sigma_k}\frac{\tilde{\rho}_w}{\langle\tilde{\rho}\rangle}\sqrt{\frac{\langle\tilde{\rho}\rangle}{\tilde{\rho}_w}} = \frac{1}{\sqrt{\langle\rho\rangle}}\frac{\mu_t}{\sigma_k},$$

respectively, such that the overall diffusion results in,

$$\frac{\partial}{\partial\hat{x}_j}\left[\left(\frac{1}{Re_\tau^\star} + \frac{\hat{\mu}_t}{\sigma_k}\right)\frac{\partial\{\hat{k}\}}{\partial\hat{x}_j}\right] = \frac{\partial}{\partial x_j}\left[\frac{1}{\sqrt{\langle\rho\rangle}}\left(\frac{\langle\mu\rangle}{Re_\tau} + \frac{\mu_t}{\sigma_k}\right)\frac{\partial\langle\rho\rangle\{k\}}{\partial x_j}\right].$$

Substituting the newly obtained terms into (3), and dividing them by $\sqrt{\langle\rho\rangle}$ to convert $t_\tau^\star$ into $t_\tau = \tilde{h}/u_\tau$, we end up with,

$$t_\tau\frac{\partial\langle\rho\rangle\{k\}}{\partial\tilde{t}} + \frac{\partial\langle\rho\rangle\{k\}\{u_j\}}{\partial x_j} = P_k - \langle\rho\rangle\varepsilon + \frac{1}{\sqrt{\langle\rho\rangle}}\frac{\partial}{\partial x_j}\left[\frac{1}{\sqrt{\langle\rho\rangle}}\left(\frac{\langle\mu\rangle}{Re_\tau} + \frac{\mu_t}{\sigma_k}\right)\frac{\partial\langle\rho\rangle\{k\}}{\partial x_j}\right]. \quad (5)$$

If compared to the conventional model for the TKE, the newly derived equation shows only one major difference that lies in the diffusion term. The diffusion term that emerges from the semi-local scaling methodology is a function of $\langle\rho k\rangle$ (instead of $\langle k\rangle$), while the diffusion coefficient and the overall diffusion term are divided by $\sqrt{\langle\rho\rangle}$. This is similar to the density corrections proposed by [10], except that in [10], only the diffusion coefficient is divided by $\langle\rho\rangle$.

3. Compressible / variable density turbulence models

The derivations described in section 2, can now be applied to various EVMs. In this work, we chose five different

Table 2: Diffusion term, normalized by viscous wall units, for the turbulent scalar equations: k, ε, ω and $\check{\nu}$ (Spalart-Allmaras variable). The differences with respect to the original model are highlight in red. σ_k, σ_ε, σ_ω, cb_2 and cb_3 are model constants. More details of turbulence models are shown in appendix A. †Catris and Aupoix [10] actually use the turbulent dissipation per unit volume as the conserved variable: $D\rho\varepsilon/Dt$.

Material derivative	Conventional	Catris & Aupoix (C&A) [10]	Present study
$\rho\frac{Dk}{Dt} = \dots$	$\frac{\partial}{\partial x_j}\left[\left(\frac{\mu}{Re_\tau}+\frac{\mu_t}{\sigma_k}\right)\frac{\partial k}{\partial x_j}\right]$	$\frac{\partial}{\partial x_j}\left[\frac{1}{\rho}\left(\frac{\mu}{Re_\tau}+\frac{\mu_t}{\sigma_k}\right)\frac{\partial \rho k}{\partial x_j}\right]$	$\frac{1}{\sqrt{\rho}}\frac{\partial}{\partial x_j}\left[\frac{1}{\sqrt{\rho}}\left(\frac{\mu}{Re_\tau}+\frac{\mu_t}{\sigma_k}\right)\frac{\partial \rho k}{\partial x_j}\right]$
†$\rho\frac{D\varepsilon}{Dt} = \dots$	$\frac{\partial}{\partial x_j}\left[\left(\frac{\mu}{Re_\tau}+\frac{\mu_t}{\sigma_\varepsilon}\right)\frac{\partial \varepsilon}{\partial x_j}\right]$	$\frac{1}{\rho}\frac{\partial}{\partial x_j}\left[\frac{1}{\sqrt{\rho}}\left(\frac{\mu}{Re_\tau}+\frac{\mu_t}{\sigma_\varepsilon}\right)\frac{\partial \rho^{1.5}\varepsilon}{\partial x_j}\right]$	$\frac{1}{\rho}\frac{\partial}{\partial x_j}\left[\frac{1}{\sqrt{\rho}}\left(\frac{\mu}{Re_\tau}+\frac{\mu_t}{\sigma_\varepsilon}\right)\frac{\partial \rho^{1.5}\varepsilon}{\partial x_j}\right]$
$\rho\frac{D\omega}{Dt} = \dots$	$\frac{\partial}{\partial x_j}\left[\left(\frac{\mu}{Re_\tau}+\frac{\mu_t}{\sigma_\omega}\right)\frac{\partial \omega}{\partial x_j}\right]$	$\frac{\partial}{\partial x_j}\left[\frac{1}{\sqrt{\rho}}\left(\frac{\mu}{Re_\tau}+\frac{\mu_t}{\sigma_\omega}\right)\frac{\partial \sqrt{\rho}\omega}{\partial x_j}\right]$	$\frac{\partial}{\partial x_j}\left[\frac{1}{\sqrt{\rho}}\left(\frac{\mu}{Re_\tau}+\frac{\mu_t}{\sigma_\omega}\right)\frac{\partial \sqrt{\rho}\omega}{\partial x_j}\right]$
$\frac{D\check{\nu}}{Dt} = \dots$	$\frac{1}{c_{b3}}\frac{\partial}{\partial x_j}\left[\left(\frac{\nu}{Re_\tau}+\check{\nu}\right)\frac{\partial \check{\nu}}{\partial x_j}\right] + \frac{c_{b2}}{c_{b3}}\left(\frac{\partial \check{\nu}}{\partial x_j}\right)^2$	$\frac{1}{\rho c_{b3}}\frac{\partial}{\partial x_j}\left[\rho\left(\frac{\nu}{Re_\tau}+\check{\nu}\right)\frac{\partial \check{\nu}}{\partial x_j} + \frac{\check{\nu}^2}{2}\frac{\partial \rho}{\partial x_j}\right] + \frac{c_{b2}}{\rho c_{b3}}\left(\frac{\partial \sqrt{\rho}\check{\nu}}{\partial x_j}\right)^2$	$\frac{1}{\rho c_{b3}}\frac{\partial}{\partial x_j}\left[\rho\left(\frac{\nu}{Re_\tau}+\check{\nu}\right)\frac{\partial \check{\nu}}{\partial x_j} + \left(\frac{\nu}{Re_\tau}+\check{\nu}\right)\frac{\check{\nu}}{2}\frac{\partial \rho}{\partial x_j}\right] + \frac{c_{b2}}{\rho c_{b3}}\left(\frac{\partial \sqrt{\rho}\check{\nu}}{\partial x_j}\right)^2$

Table 3: Channel flows investigated: $CRe^\star_\tau$ - refers to a variable property case, whose density, ρ and dynamic viscosity, μ are proportional to $1/T$ and $\sqrt{1/T}$, respectively, such that $Re^\star_\tau$ maintains constant across the channel; GL - refers to a variable property case with a gas-like density and viscosity distribution; LL - variable property case with a liquid-like viscosity distribution (density is constant); and a supersonic cases with a bulk Mach number equal to 4 from [20]. The data of the low-Mach number test cases were taken from [13]. λ is the thermal conductivity, $Re^\star_{\tau,c}$ the value of the semi-local Reynolds number at the center of the channel, Pr_w is the Prandtl number at the wall, and Φ refers to the volumetric heat source.

Channel flow	ρ/ρ_w	μ/μ_w	λ/λ_w	$Re^\star_{\tau,w}$	$Re^\star_{\tau,c}$	Pr_w	Φ
Constant $Re^\star_\tau$ ($CRe^\star_\tau$)	$(T/T_w)^{-1}$	$(T/T_w)^{-0.5}$	1	395	395	1.0	$95/(Re\ Pr_w)$
Gas-Like (GL)	$(T/T_w)^{-1}$	$(T/T_w)^{0.7}$	1	950	137	1.0	$75/(Re\ Pr_w)$
Liquid-Like (LL)	1	$(T/T_w)^{-1}$	1	150	945	1.0	$62/(Re\ Pr_w)$
Supersonic (SS)	$\propto (T/T_w)^{-1}$	$(T/T_w)^{-3/4}$	$(T/T_w)^{-3/4}$	1017	203	0.7	$Ec_\tau\left(\frac{\langle\mu\rangle}{Re_\tau}+\mu_t\right)\left(\frac{\partial\{u\}}{\partial y}\right)^2$

models (the model equations are given in Appendix A for completeness):

- the eddy viscosity correlation of Cess [15],
- the one-equation model of Spalart-Allmaras (SA) [16],
- the k-ε model of Myong and Kasagi (MK) [17],
- Menter's shear stress transport model (SST) [18],
- and the four-equations $v'^2 - f$ model (V2F) [19].

The resulting compressible / variable density modifications from the SLS approach and the density corrections proposed by [10] are indicated in red in table 2, which are mainly related to the diffusion term of the respective transport equations, the averaged operators have been omitted for brevity. Interestingly, the proposed form by [10] and the result from the SLS approach are equivalent for ε and ω, although both derivations follow alternative routes. For the SA variable, $\check{\nu}$, the only difference between our formulation and the one derived by [10] is that we include the kinematic viscosity in the density gradient term. However, this distinction is negligible, as it will be seen later. It is important to remark that the density corrections by [10] were developed following a more heuristic method than the one presented in this work. For the additional equations of the V2F model, the auxiliary transport for v'^2 has the same modifications as the modified TKE diffusion term, and the elliptic relaxation equation f does not need any modification. An additional modification we have introduced is to replace y^+ and Re_τ, e.g. within the eddy viscosity correlation of Cess and for the damping function of the MK turbulence model, by their semi-local counterparts, namely $y^\star$ and $Re^\star_\tau$ [13]. The compressible / variable density modification can also be applied to wall-modeled LES [23].

4. Fully developed channel flow

In order to test the proposed compressible / variable density modifications of the EVMs, fully developed turbulent flows in volumetrically heated channels with isothermal walls are investigated, outlined in table 3. The results are compared to direct numerical simulations performed by Patel *et al.* [14], and Trettel and Larsson [20]. For the first three cases, the density, the viscosity, and the thermal conductivity are a function of temperature only. Different constitutive relations are used that resemble behaviours of liquids, gases and fluids close to the vapour-critical point, where the case $CRe^\star_\tau$ corresponds to a fluid whose density and viscosity decrease with increasing temperature (similar to supercritical fluids), such that the semi-local Reynolds remains constant. The other cases resemble a liquid-like (LL) and gas-like (GL) behaviour, such that $Re^\star_\tau$ increases away from the wall for the liquid-like case, and $Re^\star_\tau$ decreases for the gas-like case, respectively. Due to the uniform thermal conductivity chosen in the DNS, the Prandtl number decreases away from the wall for the cases C$Re_\tau^\star$ and LL, while it increases for the GL case. The fourth case corresponds to a supersonic air flow at a bulk Mach number of $M_b = 4$ with decreasing $Re_\tau^\star$ towards the channel center and with uniform Prandtl number across the channel.

In order to model these cases, the Favre-averaged Navier-Stokes equations in Cartesian coordinates are solved in convenctional viscous wall units for the streamwise momentum and energy equations, for a fully developed flow given as

$$\frac{\partial}{\partial y}\left[\left(\frac{\langle\mu\rangle}{Re_\tau}+\mu_t\right)\frac{\partial\{u\}}{\partial y}\right] = -\left\langle \rho f_x\right\rangle, \qquad (6)$$

$$\frac{\partial}{\partial y}\left[\left(\frac{\langle\lambda\rangle}{Re_\tau Pr_w}+\frac{c_p\mu_t}{Pr_t}\right)\frac{\partial\{T\}}{\partial y}\right] = -\Phi, \qquad (7)$$

with T and λ as temperature and thermal conductivity, respectively. The flows are driven by an external body force, $\langle\rho f_x\rangle$, which for all cases is equal to τ_w/h. Moreover, the flow is heated by a volumetric source term Φ, summarized in table 3. For the supersonic case, Φ corresponds to the viscous heating, which is scaled by the Eckert number, defined as $Ec_\tau = u_\tau^2/(\tilde{T}_w\tilde{c}_{p,w})$. For an ideal gas, Ec_τ is related to the friction Mach number as $Ec_\tau = (\gamma-1)M_\tau^2$, with γ as the ratio of specific heats (for air $\gamma = 1.4$). In the low-Mach number limit, the viscous heating is negligible. Therefore, for the cases C$Re_\tau^\star$, LL, and GL, Φ is chosen as a uniform volumetric heat source, with arbitrary values such that a desired temperature difference between the channel center and the channel walls is achieved, see [14]. The reference Prandtl number is defined as $Pr_w = \tilde{\mu}_w\tilde{c}_{p,w}/\tilde{\lambda}_w$. For the low-Mach number cases, the isobaric heat capacity is taken as $c_p = \tilde{c}_p/\tilde{c}_{p,w} = 1$, while for the supersonic case, $c_p = \gamma R/(\gamma-1)$ with $R = \tilde{R}/(u_\tau^2/\tilde{T}_w)$, where $\tilde{R}$ is the specific gas constant of air. In equations (6) and (7), the Reynolds shear stress and turbulent heat flux were modelled using the Boussinesq approximation and the gradient diffusion hypothesis, respectively. In [24], it was seen that the turbulent Prandtl number, Pr_t, varies around unity for the low-Mach number cases, implying that there is a strong analogy between the momentum and scalar transport. Therefore, we have approximated $Pr_t = 1$ also for the high-Mach number case.

A no-slip condition for the velocity and equal temperatures at both channel walls are applied as boundary conditions, resulting in symmetric velocity and temperature profiles. A second order central difference scheme is used to calculate the gradients on a non-uniform mesh using exact analytic metric transformations of a hyperbolic tangent function that clusters the mesh points near the wall to ensure $y^+ \leq 1$. Mesh independent solutions were obtained for all cases on a mesh with 100 grid points. The system of equations is solved in Matlab. For more insights on the numerical solver, please refer to the source code available on Github [21] with the data for the low-Mach number cases from [14].

5. Results

The results for all EVMs are now compared with data from DNS. The velocity profiles are reported in figure 1 using the universal velocity transformation, defined in Patel *et al.* [14] as $u^\star = \int_0^{\{u^{vD}\}}\left[1+(y/Re_\tau^\star)\,\partial Re_\tau^\star/\partial y\right]\partial\{u^{vD}\}$. A more quantitative comparison with DNS is given by bar graphs in figure 2, showing the relative error of the calculated bulk Reynolds number, defined as $Re_b = u_b\rho_b h/\mu_w$, where the subscript b stands for bulk. Note, the simulations are performed by setting the friction Reynolds number. Also the temperature profiles for all cases are compared with DNS in figure 3, and the error of the Nusselt number is shown in bar graphs in figure 4. The Nusselt number is defined as $Nu = (\partial T/\partial y)_w/[(T_w - T_c)/h]$, where T_c is the temperature at the center of the channel.

In general, the compressibility / variable property modifications clearly improve the results for the velocity and temperature profiles that have been obtained by the EVMs for the cases investigated herein. The model modifications also improve the prediction of the Reynolds and Nusselt numbers for most of the cases. As can be seen, the results for the Reynolds and Nusselt number are correlated, since both the Reynolds shear stress and the turbulent heat flux have been approximated by the eddy viscosity. However, the Nusselt number estimation also depends on the choice of the turbulent Prandlt number, which has been assumed constant in this study. Because of this, the error on the Nusselt number is larger than the error on the Reynolds number for almost all investigated configurations. To verify this, closure models for the turbulent heat flux can be used to improve model results for flows with strong heat transfer [25]. As expected, figures 2 and 4 depict that for the liquid-like case (LL), for which the density is constant, the compressibility / variable property modifications do not influence the results of the SA, V2F, and SST model.

The results of each turbulence model are now analyzed individually.

- **Cess**: This eddy viscosity correlation has originally been developed by fitting experimental data of turbulent flows in pipes and is simply a function of non-dimensional wall distance and friction Reynolds number (see appendix A). Therefore, the results obtained with the unmodified Cess eddy viscosity correlation show large errors for the variable property cases. For example, the error on the Reynolds number is approximately 30% for GL, 1200% for LL, and 90% for case SS, see figure 2. However, for the variable property case with constant semi-local Reynolds number (case C$Re_\tau^\star$) the errors are only ≈2%, which confirms the fact that turbulence statistics are mainly modified by gradients in $Re_\tau^\star$ only [14].

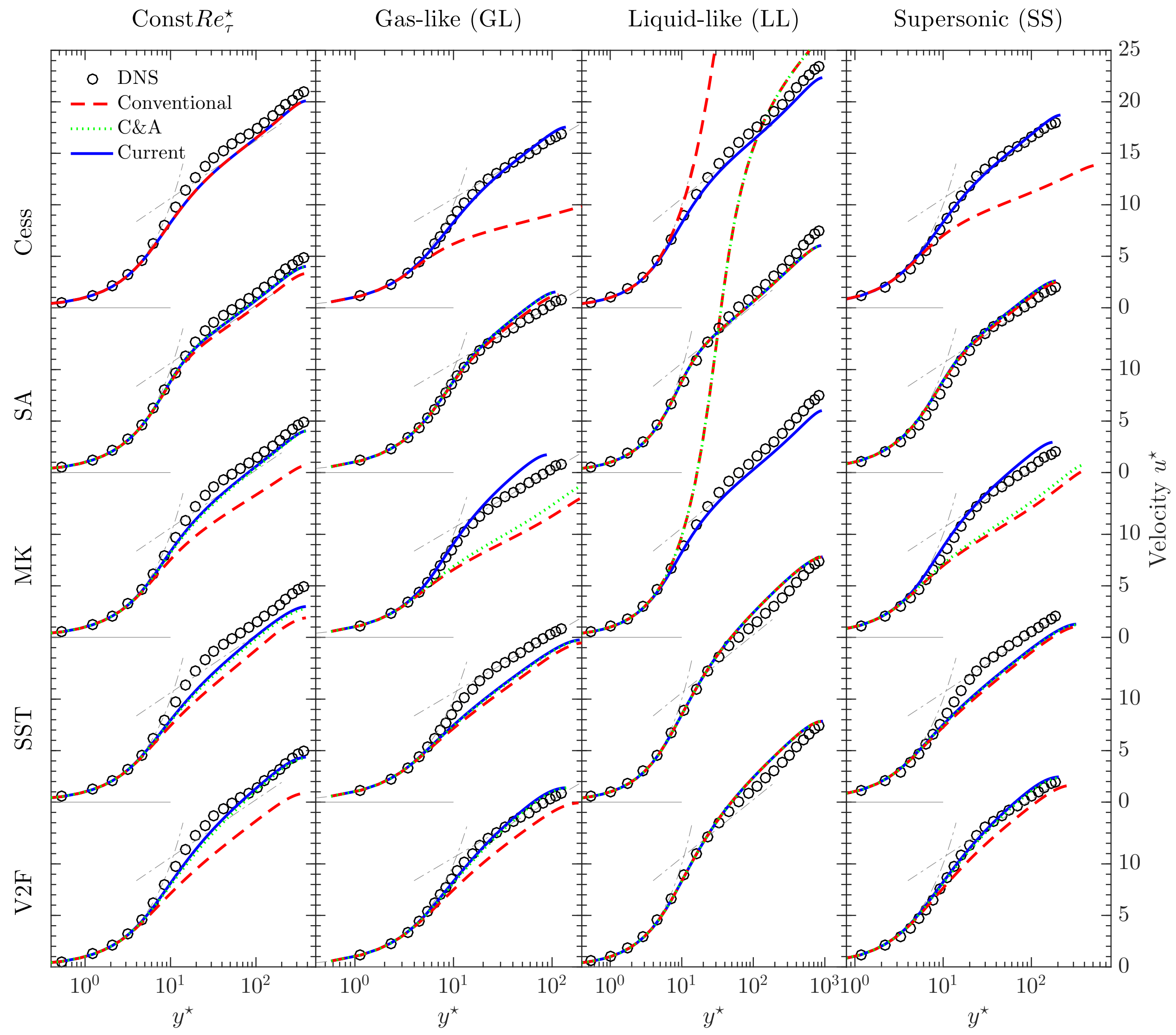

Figure 1: Turbulence model and DNS results for the velocity transformation $u^\star$ as a function of $y^\star$ for all channel flows. The grey dashed lines represent $u^\star = y^\star$ and $u^\star = 1/\kappa\ ln(y^\star) + C$, the viscous sublayer and log-law region, respectively, where $C = 5.5$.

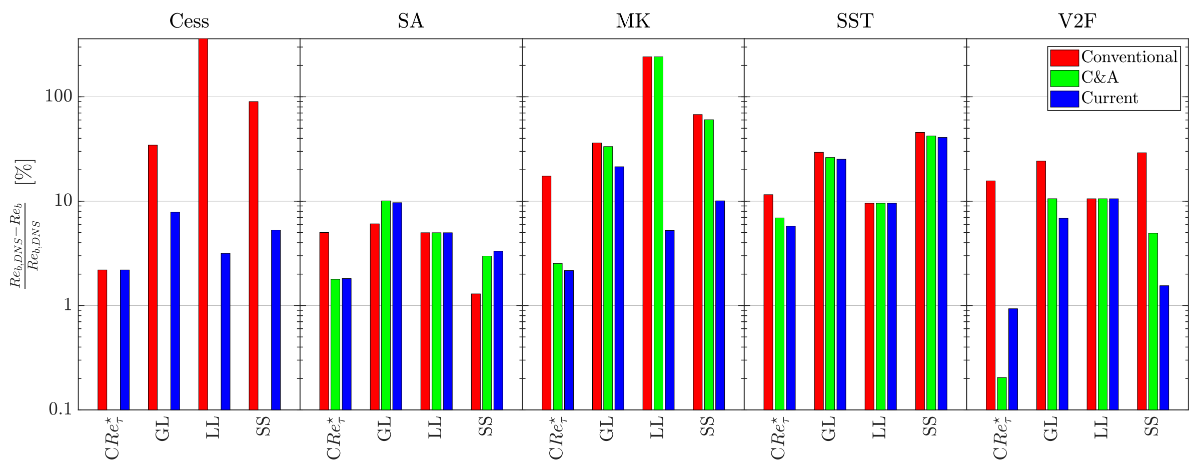

Figure 2: Relative error of the bulk Reynolds number (Re_b) calculated by models with respect to DNS data.

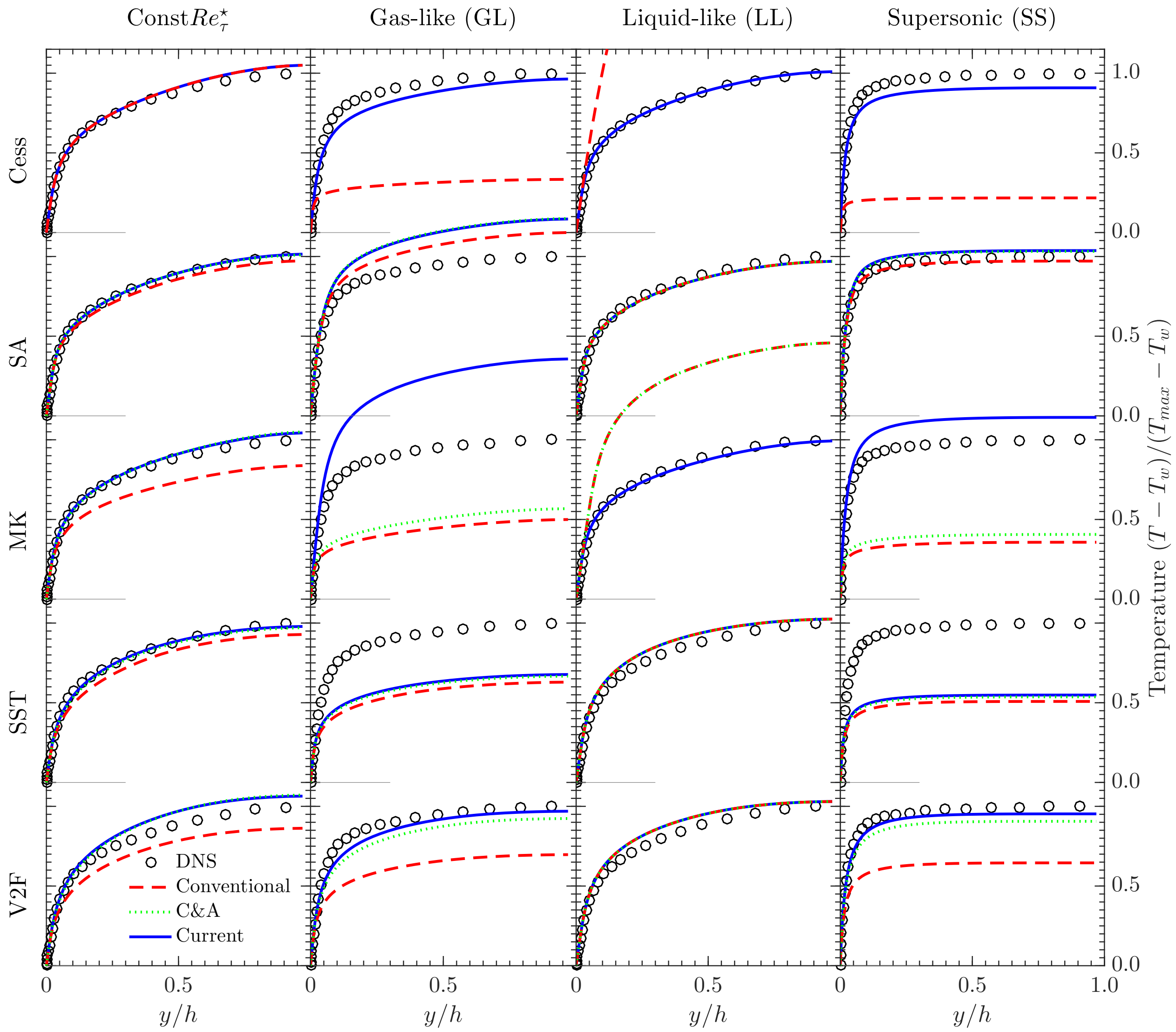

Figure 3: Turbulence model and DNS results for the scaled temperature T as a function of y/h for all channel flows.

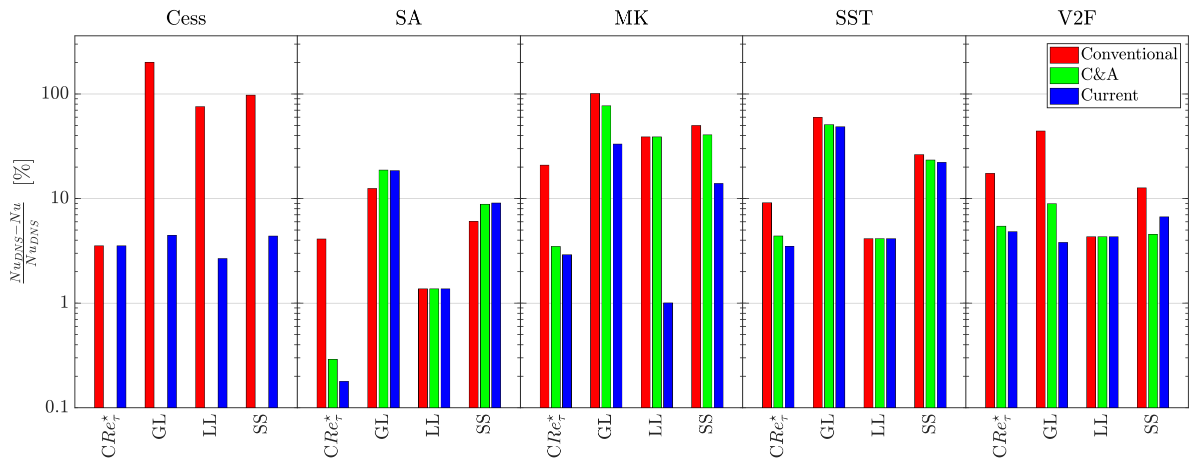

Figure 4: Relative error of the Nusselt number calculated by the models with respect to DNS data.

By simply replacing the model parameters Re_τ and y^+, by their semi-local counterparts $Re_\tau^\star$ and $y^\star$, the results for GL, LL and SS can be considerably improved (figures 1-4), again confirming that the turbulence statistics can be characterized by semi-local wall units.

- **SA**: Interestingly, the SA model accurately reproduces the velocity and temperature profiles for all variable property flows without applying any modifications, see figures 1 and 3. A further improvement, using the compressible / variable property modifications, can only be achieved for the case C$Re_\tau^\star$. For example, our proposed modification slightly improves the results for the Reynolds number (figure 2) and considerably improves the result for the Nusselt number, where the error decreases from 4% to below 0.2% (figure 4). The reason for this improvement is due to a more accurate approximation of the turbulent heat flux with the modified model. Overall, the two corrections, the one developed by [10] and the one from the SLS approach, give essentially equivalent results for the cases tested herein, see figures 1-4.

  The reason why the SA model without modifications gives more accurate results than the other models, can be explained as follows. Based on refs. [8, 14], it is apparent that the turbulent shear stress profiles collapse for turbulent flows with large variations of density and viscosity, if they are plotted as a function of $y^\star$. Using the stress balance equation, we can then also state that the viscous stresses, $\mu\ du/dy$, must collapse for variable property flows (the universal velocity transformation $u^\star$ has been derived based on this fact). Introducing the Boussinesq approximation to model the Reynolds shear stress, we can further write the stress balance as $(1+\mu_t/\mu)\mu\ du/dy = (1-y/h)$, which indicates that also the ratio of μ_t/μ must collapse for flows with variable properties. The SA model makes use of this ratio in $\chi = \check{\nu}/\nu$ (density cancels), which explains why the model performs well for all cases considered herein.

- **MK**: The largest improvements using the compressible / variable property modifications are obtained with the MK model. The effect of modifying the diffusion term and replacing y^+ with $y^\star$ in the damping function can be independently analyzed by inspecting the velocity profiles in figure 1. For case C$Re_\tau^\star$, for which $y^+ = y^\star$, the inclusion of the density in the diffusion term clearly improves the model result. On the other hand, the density correction alone does not improve the results for the other cases. For these cases, it is necessary to replace y^+ with $y^\star$ in the damping function, which can be seen by comparing the result from C&A (which still uses y^+ in the damping function) with our approach for the cases GL, LL, and SS.

- **SST**: Contrary to the other models, the SST model results do not improve substantially if used with the compressible / variable property modifications. Except for the case LL, the original model gives unsatisfactory performance with respect to the universal law of the wall, see figure 1. The modifications only slightly improve the results for the velocity profiles, as well as, reduce the errors for the Reynolds number and Nusselt number. The only case that shows an improvement is the C$Re_\tau^\star$, see figures 1 and 3. By further investigating the results, it can be seen that the blending function of this model is equal to 1 across the channel height, since the test cases simulated herein have a low Reynolds number. Therefore, the model essentially solves the standard k-ω model [26]. It was also seen by [10], that the density correction of the diffusion term has little effect on the flow field predictions for the k-ω model.

- **V2F**: This model with the compressible / variable property modifications improves the collapse with the DNS data if compared to the conventional form for cases C$Re_\tau^\star$, GL, and SS. These results are consistent with the ones presented in Pecnik and Patel [13], who solved the V2F model in semi-locally scaled form. In contrast, the present study also solved the energy equation.

6. Conclusion

Based on the semi-locally scaled TKE equation, we have derived a novel methodology to improve eddy viscosity models for predicting wall-bounded turbulent flows with strong variations in thermo-physical properties. The major difference of the new methodology is the formulation of the diffusion term in the turbulence scalar equations. For example, the modified diffusion term of the turbulent kinetic energy equation reads, $\tilde{\rho}^{-0.5}\partial_{\tilde{x}}\left[\tilde{\rho}^{-0.5}\left(\tilde{\mu}+\tilde{\mu}_t\right)\left(\partial_{\tilde{x}}\tilde{\rho}\tilde{k}\right)\right]$ (averaging operators omitted). Common compressibility terms, such as; dilatation diffusion, pressure work, and pressure dilation, are not taken into account in the modified TKE equation. This derived methodology is generic and applicable to several turbulent scalars and it can also be applied to wall-modeled LES. In general, the modified EVMs result in a better agreement with the DNS data in terms of velocity profiles and heat transfer of fully developed turbulent channel flows with variable property fluids. Interestingly, the standard Spalart-Allmaras model, originally developed for external flow, gives the most reliable results, with respect to other conventional EVM, for the variable property cases investigated herein.

Future studies will include the implementation of the modified turbulence models to more complex flow configurations, e.g. turbulent pipe flow with a fluid undergoing heat transfer at supercritical pressure.

7. Acknowledgements

The authors thank the Netherlands Organization for Scientific Research (NWO) who funded this research through the grant with project number 14711. We also acknowledge Andrew Trettel and Johan Larsson for providing the data for the fully developed supersonic turbulent channel flow.

Appendix A: Eddy viscosity models

Cess' eddy viscosity correlation

In 1958, Cess [15] developed a correlation for the effective viscosity ($\mu + \mu_t$) in fully developed turbulent pipe flows. It combines a van Driest [27] type damping function for the laminar sublayer with the outer layer solution proposed by Reichardt [28]. The correlation was later extended for channel flows by Hussain and Reynolds [29], which reads for a channel whose walls are located at $y_w = 0$ and $y_w = 2$, as

$$\frac{\mu_t}{\mu} = \frac{1}{2}\left[1 + \frac{\kappa^2 Re_\tau^2}{9}\left(2y_w - y_w^2\right)^2\left(3 - 4y_w - y_w^2\right)^2 \left(1 + e^{-y^+/A^+}\right)^2\right]^{1/2} + \frac{1}{2},$$

with the normalized wall distance $y_w = \tilde{y}_w/\tilde{h}$, $A^+ = 25.4$, and $\kappa = 0.41$ the von Karman constant.

Spalart-Allmaras turbulence model

The Spalart-Allmaras (SA) model is a one equation turbulence model, derived on the basis of dimensional analysis, Galilean invariance and empiricism [16]. The standard form of the SA model reads

$$\frac{\partial \check{\nu}}{\partial t} + u_j\frac{\partial \check{\nu}}{\partial x_j} = c_{b1}\check{S}\check{\nu} - c_{w1}f_w\left(\frac{\check{\nu}}{y_w}\right)^2 + \frac{c_{b2}}{c_{b3}}\left(\frac{\partial \check{\nu}}{\partial x_j}\right)^2 + \frac{1}{c_{b3}}\frac{\partial}{\partial x_j}\left[\left(\frac{\nu}{Re_\tau} + \check{\nu}\right)\frac{\partial \check{\nu}}{\partial x_j}\right].$$

The model functions are:

$$\check{S} = S + \frac{\check{\nu}}{\kappa^2 {y_w}^2}f_{v2},\ f_{v2} = 1 - \frac{\chi}{1+\chi f_{v1}},\ f_{v1} = \frac{\chi^3}{\chi^3 + c_{v1}^3},$$

$$\chi = \frac{\check{\nu}}{\nu},\ f_w = g\left[\frac{1+c_{w3}^6}{g^6 + c_{w3}^6}\right]^{1/6},\ g = r + c_{w2}(r^6 - r),$$

$$r = \frac{\check{\nu}}{\check{S}\kappa^2 {y_w}^2}.$$

where the modulus of the strain rate tensor is $S = \sqrt{2S_{ij}S_{ij}}$, with $S_{ij} = \frac{1}{2}\left(\partial u_i/\partial x_j + \partial u_j/\partial x_i\right)$. The eddy viscosity is modelled as

$$\mu_t = \rho\check{\nu}f_{v1}.$$

The model coefficient are: $c_{b1} = 0.1355$, $c_{b2} = 0.622$, $c_{b3} = 2/3$, $c_{v1} = 7.1$, $c_{w1} = c_{b1}/\kappa^2 + (1 + c_{b2})/c_{b3}$, $c_{w2} = 0.3$, $c_{w3} = 2$ and the von Karman constant $\kappa = 0.41$. The wall boundary condition is $\check{\nu}_w = 0$.

Myong and Kasagi model

Myong and Kasagi (MK) model [17] is a low-Reynolds k-ϵ model, given as

$$\frac{\partial \rho k}{\partial t} + \frac{\partial \rho k u_j}{\partial x_j} = P_k - \rho\varepsilon + \frac{\partial}{\partial x_j}\left[\left(\frac{\mu}{Re_\tau} + \frac{\mu_t}{\sigma_k}\right)\frac{\partial k}{\partial x_j}\right],$$

$$\frac{\partial \rho \varepsilon}{\partial t} + \frac{\partial \rho \varepsilon u_j}{\partial x_j} = C_{\varepsilon 1}P_k\frac{\varepsilon}{k} - C_{\varepsilon 2}f_\varepsilon\rho\frac{\varepsilon^2}{k} + \frac{\partial}{\partial x_j}\left[\left(\frac{\mu}{Re_\tau} + \frac{\mu_t}{\sigma_\varepsilon}\right)\frac{\partial \varepsilon}{\partial x_j}\right],$$

where, P_k is the production of TKE using the Boussinesq approximation. The functions and the eddy viscosity are given as:

$$f_\varepsilon = \left[1 - \frac{2}{9}e^{\left[-\left(\frac{Re_t}{6}\right)^2\right]}\right]\left[1 - e^{\left(-\frac{y^+}{5}\right)}\right]^2,$$

$$f_\mu = \left[1 - e^{\left(-\frac{y^+}{70}\right)}\right]\left[1 + \frac{3.45}{\sqrt{Re_t}}\right],$$

$$\mu_t = C_\mu f_\mu \rho\frac{k^2}{\varepsilon},$$

with $Re_t = \rho k^2/\mu\varepsilon$ and $y^+ = yRe_\tau$. The model constants are: $C_{\varepsilon 1} = 1.4$, $C_{\varepsilon 2} = 1.8$, $C_\mu = 1.4$, $\sigma_k = 1.4$, and $\sigma_\varepsilon = 1.3$. Finally, the wall boundary conditions for the scalars are

$$k_w = 0,\ \varepsilon_w = \frac{\mu_w}{\rho_w}\frac{\partial^2 k}{\partial y^2}\bigg|_w \approx \frac{2\mu_w k_1}{\rho_w y_1^2}.$$

Menter Shear Stress Transport (SST) model

Menter's SST model [18] is given as

$$\frac{\partial \rho k}{\partial t} + \frac{\partial \rho k u_j}{\partial x_j} = P_k^{\lim} - \beta^\star\rho k\omega + \frac{\partial}{\partial x_j}\left[\left(\frac{\mu}{Re_\tau} + \sigma_k\mu_t\right)\frac{\partial k}{\partial x_j}\right],$$

$$\frac{\partial \rho \omega}{\partial t} + \frac{\partial \rho \omega u_j}{\partial x_j} = \frac{\alpha\rho}{\mu_t}P_k - \beta\rho\omega^2 + (1 - F_1)\,CD_{k\omega} + \frac{\partial}{\partial x_j}\left[\left(\frac{\mu}{Re_\tau} + \sigma_\omega\mu_t\right)\frac{\partial \omega}{\partial x_j}\right],$$

with $P_k^{\lim} = min\left(P_k, 20\beta^\star\rho\omega k\right)$, and

$$CD_{k\omega} = 2\frac{\rho\sigma_{\omega 2}}{\omega}\frac{\partial k}{\partial x_j}\frac{\partial \omega}{\partial x_j}.$$

The blending functions and the eddy viscosity are given by:

$$F_1 = tanh\left[\left(min\left[max\left(\gamma_1, \gamma_2\right), \gamma_3\right]\right)^4\right],$$

$$F_2 = tanh\left[\left(max\left(2\ \gamma_1, \gamma_2\right)\right)^2\right],$$

$$\gamma_1 = \frac{\sqrt{k}}{\beta^\star \omega y},\ \gamma_2 = \frac{500\mu}{\rho y_w^2 \omega},\ \gamma_3 = \frac{4\rho\sigma_{\phi 2} k}{y_w^2\ max\left(CD_{k\omega}, 10^{-20}\right)},$$

$$\mu_t = \frac{\rho C_\mu k}{max\left(C_\mu \omega, \Omega F_2\right)},$$

with Ω the vorticity magnitude. The model coefficient are $\beta^\star = 0.09$, $C_\mu = 0.31$. The other model coefficient are calculated with the blending function F_1 using the relation $C = F_1 C_1 + (1 - F_1) C_2$, with $\beta_1 = 0.075$, $\beta_2 = 0.0828$, $\sigma_{k1} = 0.85$, $\sigma_{k2} = 0.5$, $\sigma_{\omega 1} = 1.0$, $\sigma_{\omega 2} = 0.856$, $\alpha_1 = \beta_1/\beta^\star - \sigma_{\omega 1}\kappa^2/\sqrt{\beta^\star}$, and $\alpha_2 = \beta_2/\beta^\star - \sigma_{\omega 2}\kappa^2/\sqrt{\beta^\star}$. Finally, the wall boundary condition are

$$k_w = 0,\ \omega_w = \frac{60\mu_w}{\rho_w \beta_1 {y_w}^2}.$$

Durbin's v'^2-f model

Durbin's v'^2-f model [19] is a k-ϵ model with an additional transport equation for the wall-normal velocity fluctuation v'^2, and an elliptic relaxation equation f that models the pressure strain correlation for v'^2. The model equations are given as:

$$\frac{\partial \rho k}{\partial t} + \frac{\partial \rho k u_j}{\partial x_j} = P_k - \rho\varepsilon + \frac{\partial}{\partial x_j}\left[\left(\frac{\mu}{Re_\tau} + \frac{\mu_t}{\sigma_k}\right)\frac{\partial k}{\partial x_j}\right],$$

$$\frac{\partial \rho\varepsilon}{\partial t} + \frac{\partial \rho\varepsilon u_j}{\partial x_j} = \frac{1}{T_t}\left[C_{\varepsilon 1}\left(1 + 0.045\sqrt{\frac{k}{v'^2}}\right)P_k - C_{\varepsilon 2}\rho\varepsilon\right] + \frac{\partial}{\partial x_j}\left[\left(\frac{\mu}{Re_\tau} + \frac{\mu_t}{\sigma_\varepsilon}\right)\frac{\partial \varepsilon}{\partial x_j}\right],$$

$$\frac{\partial \rho v'^2}{\partial t} + \frac{\partial \rho v'^2 u_j}{\partial x_j} = \rho k f - N\frac{\rho v'^2}{k}\varepsilon + \frac{\partial}{\partial x_j}\left[\left(\frac{\mu}{Re_\tau} + \mu_t\right)\frac{\partial v'^2}{\partial x_j}\right],$$

$$f - L_t^2 \Delta f = \left(C_{f1} - 1\right)\frac{2/3 - v'^2/k}{T_t} - C_{f2}\frac{P_k}{\rho k} + \left(N - 1\right)\frac{v'^2}{k T_t}.$$

The turbulent time and length scale, and the eddy viscosity are modelled as,

$$T_t = max\left(\frac{k}{\varepsilon}, 6\sqrt{\frac{\mu}{\rho\varepsilon}}\right),$$

$$L_t = 0.23\ max\left(\frac{k^{3/2}}{\varepsilon},\ 70\left(\frac{\mu^3}{\rho^3\varepsilon}\right)^{1/4}\right),$$

$$\mu_t = C_\mu \rho v'^2 T_t.$$

The model closure coefficient are $C_{\varepsilon 1} = 1.4$, $C_{\varepsilon 2} = 1.9$, $C_\mu = 0.22$, $C_{f1} = 1.4$, $C_{f2} = 0.3$ and $N = 6$. Finally, the wall boundary conditions are

$$k_w = 0,\ \varepsilon_w = \frac{\mu_w}{\rho_w}\frac{\partial^2 k}{\partial y^2}\bigg|_w,\ v_w'^2 = 0,\ f_w = 0.$$

References

[1] P. Bradshaw, Compressible turbulent shear layers, Annual Review of Fluid Mechanics 9 (1) (1977) 33–52.

[2] L. Duan, I. Beekman, M. P. Martin, Direct numerical simulation of hypersonic turbulent boundary layers. Part 2. Effect of wall temperature, Journal of Fluid Mechanics 655 (May) (2010) 419–445.

[3] J. Lee, S. Y. Jung, H. J. Sung, T. A. Zaki, Effect of wall heating on turbulent boundary layers with temperature-dependent viscosity (2013) 196–225.

[4] D. Modesti, S. Pirozzoli, Reynolds and Mach number effects in compressible turbulent channel flow, International Journal of Heat and Fluid Flow 59 (2016) 33–49.

[5] P. G. Huang, P. Bradshaw, T. J. Coakely, Turbulence models for compressible boundary layers, AIAA Journal 32 (4) (1994) 735–740.

[6] S. Sarkar, G. Erlebacher, M. Hussaini, H. Kreiss, The analysis and modelling of dilatational terms in compressible turbulence, Journal of Fluid Mechanics 227 (1991) 473–493.

[7] O. Zeman, A new model for super/hypersonic turbulent boundary layers, in: 31st Aerospace Sciences Meeting, 1993, p. 897.

[8] P. Huang, P. G., Coleman, G. N., Bradshaw, Compressible Turbulent channel flows, DNS results and modelling, JFM (1995) (1995) 185–218.

[9] E. Van Driest, Journal of the Aeronautical Sciences, Journal Of The Aeronautical Sciences 40 (6) (1951) 145–160.

[10] S. Catris, B. Aupoix, Density corrections for turbulence models, Aerospace Science and Technology 4 (1) (2000) 1–11.

[11] F. Roy, C., Blottner, Review and assessment of turbulence models for hypersonic flows 42 (2006) (2007) 469–530.

[12] A. J. Smits, J.-P. Dussauge, Turbulent shear layers in supersonic flow, Springer Science & Business Media, 2006.

[13] R. Pecnik, A. Patel, Scaling and modelling of turbulence in variable property channel flows, Journal of Fluid Mechanics 823.

[14] A. Patel, B. J. Boersma, R. Pecnik, The influence of near-wall density and viscosity gradients on turbulence in channel flows, Journal of Fluid Mechanics 809 (2016) 793–820.

[15] R. Cess, A survey of the literature on heat transfer in turbulent tube flow, Res. Rep (1958) 8–0529.

[16] P. R. Spalart, S. R. Allmaras, et al., A one equation turbulence model for aerodynamic flows, RECHERCHE AEROSPATIALE-FRENCH EDITION- (1994) 5–5.

[17] N. Myong, H.K. and Kasagi, A New Approach to the Improvement of k-e turbulence model for wall-bounded shear flows, JSME 33 (2).

[18] F. R. Menter, Zonal Two Equation k-w, Turbulence Models for Aerodynamic Flows, AIAA paper (1993) 2906.

[19] P. A. Durbin, Separated Flow Computations with the k-e-v2 Model, AIAA Journal 33 (4) (1995) 659–664.

[20] A. Trettel, J. Larsson, Mean velocity scaling for compressible wall turbulence with heat transfer, Physics of Fluids 28 (2) (2016) 026102.

[21] R. Pecnik, G. Otero Rodriguez, A. Patel, RANS-models for fully developed turbulent channel

flow with variable properties solved in Matlab, https://github.com/Fluid-Dynamics-Of-Energy-Systems-Team/RANS_Channel (2018).

[22] P. Bradshaw, J. B. Perot, A note on turbulent energy dissipation in the viscous wall region, Physics of Fluids A: Fluid Dynamics (1989-1993) 5 (12) (1993) 3305–3306.

[23] A. Patel, R. Pecnik, J. Peeters, S. Hickel, M. Moghadam, Turbulence modulation by variable density and viscosity, in: Proceedings of the Summer Program, 2016, p. 213.

[24] A. Patel, B. J. Boersma, R. Pecnik, Scalar statistics in variable property turbulent channel flows, Physical Review Fluids 2 (8) (2017) 084604.

[25] V. Boutrouche, E. Franquet, S. Serra, R. Manceau, Influence of the turbulence model for channel flows with strong transverse temperature gradients, International Journal of Heat and Fluid Flow 70 (2018) 79–103.

[26] D. C. Wilcox, et al., Turbulence modeling for CFD, Vol. 2, DCW industries La Canada, CA, 1998.

[27] E. R. Van Driest, On turbulent flow near a wall, J. Aeronaut. Sci 23 (11) (1956) 1007–1011.

[28] H. Reichardt, Vollständige darstellung der turbulenten geschwindigkeitsverteilung in glatten leitungen, ZAMM-Journal of Applied Mathematics and Mechanics/Zeitschrift für Angewandte Mathematik und Mechanik 31 (7) (1951) 208–219.

[29] A. K. M. F. Hussain, W. C. Reynolds, Measurements in Fully Developed Turbulent Channel Flow, Journal of Fluids Eng. (7).